

3D NUMERICAL SIMULATION INVESTIGATING THE EFFECT OF VOLUMETRIC FLOW RATE ON CORE DEFLECTION

Ya-Yuen Chou¹, Wen-Hsien Yang¹, and A. J. Giacomini², A. J. Hade²

1. CoreTech System (Moldex3D) Co., Ltd., ChuPei City, Hsinchu, Taiwan

2. Rheology Research Center and Mechanical Engineering Department, University of Wisconsin, Madison Wisconsin, USA 53706

Abstract

Core deflection results from an unevenly advancing melt front around long slender cores during injection molding. It is a pervasive problem in the manufacturing of long slender hollow parts, especially when they are thin-walled. Core deflection not only causes uneven wall thickness, but also affects the melt flow. In this paper, an effective 3D numerical approach is developed to simulate the flow around a cantilevered core, to calculate the uneven pressure distribution around the core, and to predict the core deflection. Moreover, the relation between volumetric flow rate and core deflection will be compared with a recent analytical solution (Giacomini and Hade, 2005).

Introduction

When injection molding long slender hollow parts with one closed end, cantilevered cores arise raising manufacturing challenges. The unevenly advancing melt front around such cores, inevitable during injection molding, causes core deflection. It is a pervasive problem in the manufacturing of long slender hollow parts, and especially when they are thin-walled. Where its deflection causes the core to touch the cavity wall, a hole will perforate the part. Therefore, mold designers are interested in the maximum core deflection to prevent this. In this study, an effective 3D numerical approach is developed to simulate the flow around a cantilevered core and is able to predict the core deflection by linking the flow analysis to the stress analysis. We validate the new simulation with a recent analytical solution (Giacomini and Hade, 2005).

Conventional 2.5D CAE molding analysis adopts the *mid-plane model*, replacing the flow geometry with analysis along its midplane. This technology is now mature, computationally efficient and accurate, especially for thin-walled plastic parts. This is why 2.5D analysis is now so widely used in injection molding. For the more complicated problem of core deflection, we prefer to depart from the mid-plane model. Here, we

develop a 3-dimensional numerical approach to simulate the uneven flow and pressure around core components during mold filling and we further predict the corresponding core deflection.

Theory

Analytical Solution [5]:

Fig. 1 illustrates a cantilevered core of constant rectangular cross-section. We restrict our worst case analysis to the Newtonian fluid, conservatively neglecting its solidification. Accordingly, we consider the mold filling very unevenly, with the polymer flowing down just one side of the mold. Giacomini and Hade studied this problem analytically and discovered that core deflection is governed by the dimensionless volumetric flow rate Q which they called *core deflectability*. The dimensionless core deflection Y and Q are related by:

$$\frac{d^5 Y}{dX^5} = \frac{-12Q}{(1+Y)^3} \quad (1)$$

where:

$$Q \equiv \frac{\mu QL}{EI} \left(\frac{L}{B_0} \right)^4 \quad (2)$$

and where μ is Newtonian viscosity, Q is volumetric flow rate, L is core length, EI is the core stiffness, and B_0 is the gap between the mold wall and the core base.

Dimensionless core deflection is defined by:

$$Y \equiv \frac{y}{B_0} \quad (3)$$

where y is core deflection, and the dimensionless axial position along core X is defined by

$$X \equiv \frac{x}{L} \quad (4)$$

Three-Dimensional Numerical Approach

In this study, the melt flow pressure during filling is predicted by the following numerical solution. The governing equations to simulate transient, non-isothermal 3D flow are:

$$\frac{\partial \rho}{\partial t} + \nabla \cdot \rho \mathbf{u} = 0 \quad (5)$$

$$\frac{\partial}{\partial t} (\rho \mathbf{u}) + \nabla \cdot (\rho \mathbf{u} \mathbf{u} - \boldsymbol{\sigma}) = \rho \mathbf{g} \quad (6)$$

$$\boldsymbol{\sigma} = -p \mathbf{I} + \eta (\nabla \mathbf{u} + \nabla \mathbf{u}^T) \quad (7)$$

$$\rho C_p \left(\frac{\partial T}{\partial t} + \mathbf{u} \cdot \nabla T \right) = \nabla \cdot (\mathbf{k} \nabla T) + \eta \dot{\gamma}^2 \quad (8)$$

where \mathbf{u} is the velocity vector, T is the temperature, t is the time, p is the pressure, $\boldsymbol{\sigma}$ is the total stress tensor, ρ is the fluid density, η is the viscosity, \mathbf{k} is the thermal conductivity, C_p is the specific heat, and $\dot{\gamma}$ is the magnitude of the rate of deformation tensor.

The melt pressure p during filling is governed by Eq. (7). Moreover, it exerts a net lateral force on the core surface. Hence the core deflection can be obtained from the force balance:

$$\nabla \boldsymbol{\sigma} + \mathbf{F} = 0 \quad (9)$$

where $\boldsymbol{\sigma}$ is the stress and \mathbf{F} is the body force from melt pressure.

The finite volume method (FVM) due to its robustness and efficiency is employed in this study to solve the transient flow field in complex three-dimensional geometries. In FVM, to discretize the equations, the whole computational domain is subdivided into a finite number of non-overlapping control volumes. The transport variables are stored at the centroid of each control volume. The transport equations are then integrated over each of the control volumes in the domain. The central differencing scheme is combined with the upwind scheme to approximate the transport variables at the cell faces. This solver has been successfully applied in injection molding filling simulation [3]. Numerical experiments confirm the reliability and efficiency of the solver.

Results and discussions

To validate our core deflection simulation, we compare with a recent analytical solution (Giacomin and Hade, 2005) [5]. Since the analytical solution employs proposed under several assumptions, we simplify our 3-dimensional simulation accordingly, first by adopting a symmetric pressure distribution along thickness direction during filling. We then restrict our analysis to a temperature-independent Newtonian melt. Since polymer flowing down just one side of the core was considered in the analytical solution, we use the pressure loading when the mold fills with the polymer just flowing down beneath the slender core as the initial condition for our stress analysis. Since solidification was neglected in the analytical solution, we output the simulation results of filling analysis to the sequential stress solver. Eq. (8) incorporates heat transfer between the hot melt and the cold mold (including the cold core), whereas the analytical solution is for the much simpler isothermal problem. Finally, whereas Eq. (8) accounts for viscous heating, the analytical solution to which our results are compared does not.

Fig. 1 illustrates our 3-dimensional model whose specific dimensions are chosen arbitrarily (see Fig. 2 (a) and (b)) for comparison with a dimensionless analytical solution for core deflection. Table 1 lists the core material, its elastic modulus and its moment, along with the molding conditions. We use these data as the simulation conditions for filling and core deflection analysis, and then change the filling time to explore different flow rates. As the polymer on just one side of the mold reaches the end of the slender core, the pressure loading on the core exerted by this fluid is output as the boundary condition for the subsequent stress analysis (see Fig. 3(a)).

Here we consider the two most common cantilevered core conditions. Case 1 is with a free core tip, gated near this tip. Case 2 is also with a free core tip, but gated near its base. Were these cores undeflected, for both Cases 1 and 2, the pressure loadings on the slender cores would mirror one another. Thus, to approach the analytical solution, we use the two constraints shown in Fig. 4 to simulate Case 1 and Case 2 in the stress analyses. After these stress analyses complete, the maximum core deflection arising at the core's free end is obtained for each different flow rate.

Table 2 lists the simulated maximum core deflection change for different flow rates. Fig. 5 compares the simulation and the analytical results and shows that these agree closely in the linear regime, where $Q \leq 0.1$. However, we also find that the simulations fail to capture the nonlinearity for higher values of Q . This is because the effect of core

deflection on flow pressure is not considered in our simulations.

Moreover, in our 3-dimensional numerical approach for core deflection prediction, we can compute the core deformation and its stress distribution at different times during filling. We can thus explore the effect of the unevenly advancing melt front on the developing deflection. Take the base-gated Run 3 ($Q = 0.01$) for example. Fig.6 (a) and (b) show the melt front position and the pressure distribution at different times during filling. The pressure loading on the cantilevered core at each time is then output to the stress solver, after stress analysis completes; Fig.6 (c) and (d) show the corresponding Von Mises stress and the deformed shape of the cantilevered core. From these figures, we can see that the unevenly advancing melt front around the core strongly affects core deflection. As the amount of polymer injected into cavity increases, the stress and deflection of core also increases. However, as polymer reaches another side of the core, the maximum stress and deflection of core decreases since pressure exerted by fluid on the top to core increases.

Conclusion

A 3-dimensional numerical approach is developed to simulate the flow around a cantilevered core and it accurately predicts core deflection by linking the flow analysis to the core stress analysis. The simulation is validated by its close agreement with a recent analytical solution (Giacomin and Hade, 2005), especially at low flow rate, where core deflection varies linearly with the injection flow rate.

Reference

- [1]. E.C. Bernhardt (Ed.), Computer Aided Engineering for Injection Molding, Hanser (1983)
- [2]. T.A. Shepard, M. O'Connell, K. Powell and S. Charwinsky, "Minimizing Coreshift In Injection Moulded Containers", *Plastics Engineering*, **52**(2), 27-29 (1996).
- [3]. R.Y. Chang and W.H. Yang, *Int. J. Numer. Methods Fluids*, **37**, 125-148 (2001).
- [4]. R.Y. Chang and W.H. Yang, "A Novel Three-Dimensional Analysis of Polymer Injection Molding", 740, ANTEC 2001, Dallas (2001).
- [5]. A.J. Giacomin and A.J. Hade, "Core Deflection in Injection Molding", 461, *Advanced Forming Technology*, 2005.

Key Words

Core deflection, core deflectability, thin-walled injection molding.

Table 1 Polymer, core properties and molding conditions

Molding Conditions	
Polymer	ABS STYLAC VA29
Core Material Name	Copper
Melt Temperature	225°C
Mold Temperature	60°C
Core Elastic Modulus	1.15×10^{12} dyne/cm ²
Core Moment of Inertia	0.16276 cm ⁴

Table 2 Peak dimensionless core deflection at different dimensionless flow rates

Run No.	Dimensionless Flow Rate Q	Flow Rate Q (cm ³ /sec)	Viscosity (g/cm·s)	Simulation Results: Dimensionless Core Deflection Y	
				Core tip	Core base
1	0.0001	4.53647	69.8947	0.0001032	4.18692E-05
2	0.001	45.3647	69.8947	0.0010359	0.000420935
3	0.01	453.647	69.8947	0.0107747	0.004414579
4	0.1	9.85723	32166.8	0.1484112	0.05686271
5	1	98.5723	32166.8	1.0314953	0.418504673
6	10	985.723	32166.8	10.316636	4.186448598
7	100	9857.23	32166.8	103.36449	46.63738318

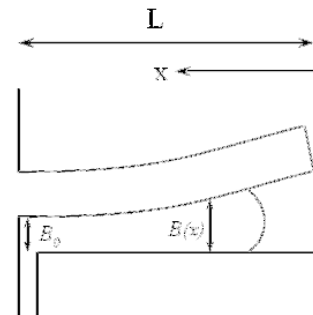
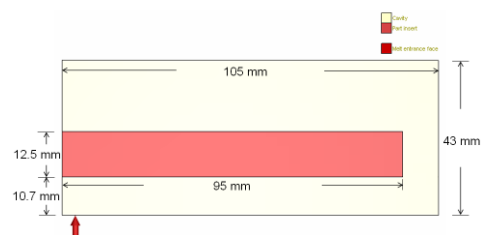
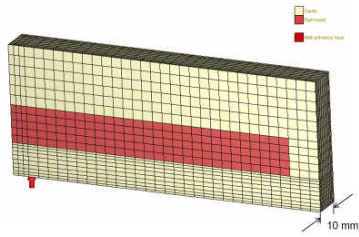


Fig.1 Schematic of base-gated core deflection [5].

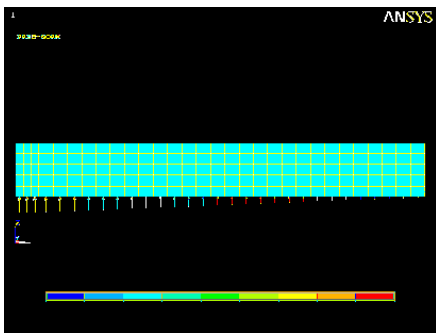


(a) Part shape and thickness

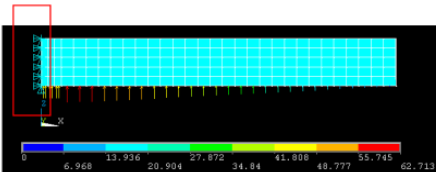


(b) Solid mesh of cavity and slender core

Fig.2 Model geometry: (a) Part shape and thickness (b) Solid mesh of cavity and slender core



(a) Initial pressure condition



(b) Fixed displacement (tip-gated)

Fig. 3 Boundary condition settings in stress analysis

(a) Initial pressure condition

(b) Fixed displacement (tip-gated)

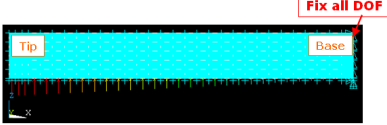
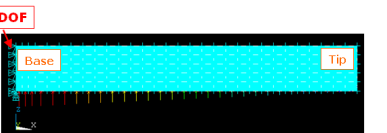
- Case 1: 
- Gated near the tip
- Case 2: 
- Gated near the base

Fig.4 Settings for fixed displacement of Cases 1 and 2

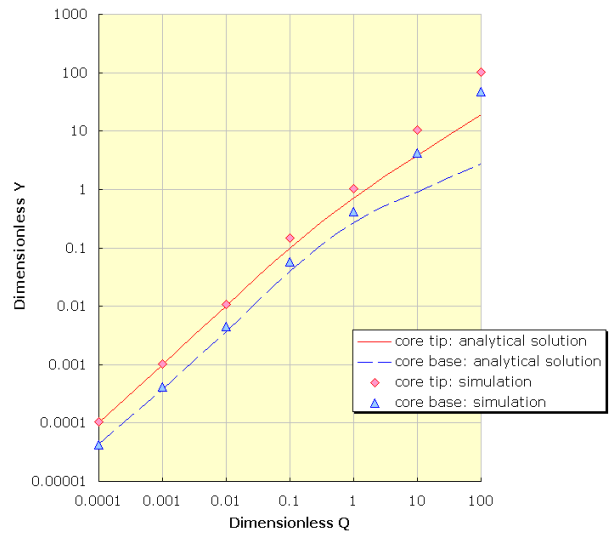
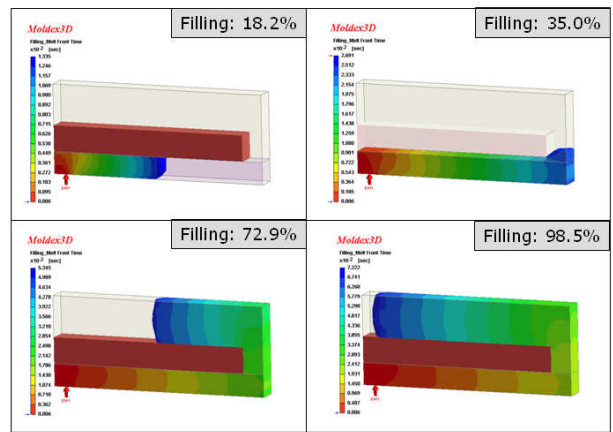
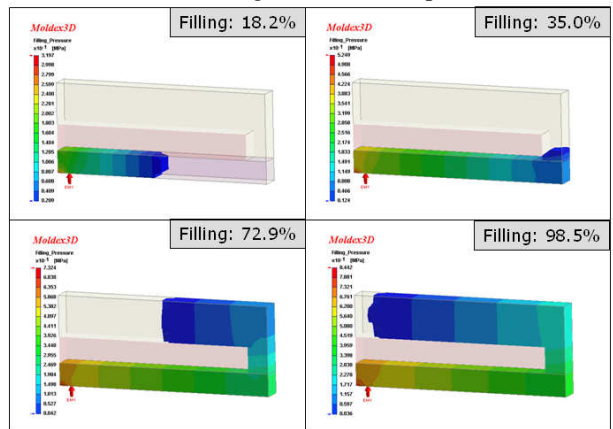


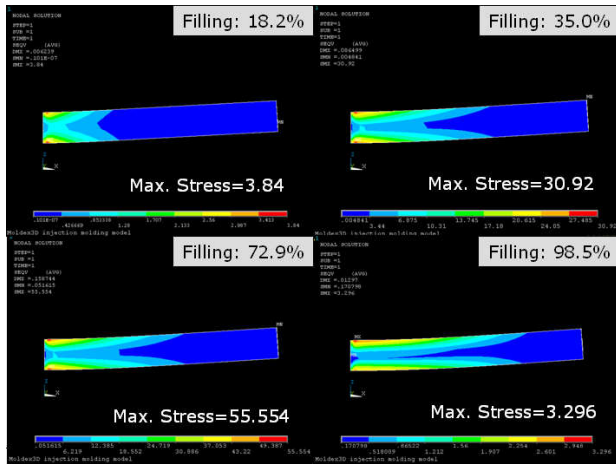
Fig. 5 Comparing numerical simulation with analytical solution



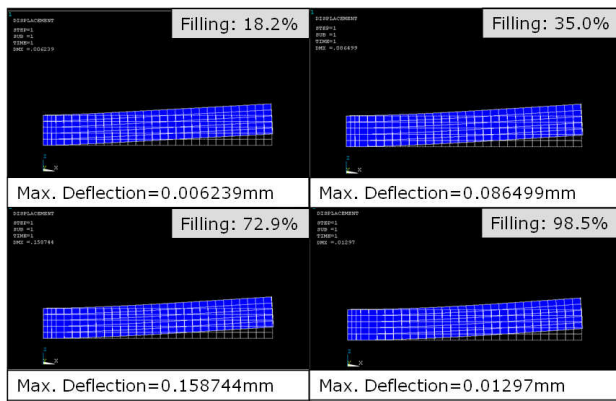
(a) Filling: Melt front shape



(b) Filling: Pressure distribution



(c) Von Mises Stress



(d) Deformed shape

Fig. 3 Multiple time steps (a) Melt front (b) Pressure distribution (c) Von Mises Stress (d) Deformed core shape